Sensors & Diagnostics

PAPER

View Article Online
View Journal | View Issue

Cite this: *Sens. Diagn.*, 2023, **2**, 938

Ion-transfer electroanalytical detection of perfluorooctanoic acid at a liquid–liquid micro-interface array†

Hum Bahadur Lamichhane and Damien W. M. Arrigan *

Received 6th April 2023,
Accepted 22nd June 2023

DOI: 10.1039/d3sd00080j

rsc.li/sensors

Per- and polyfluoroalkyl substances (PFAS) are synthetic materials that bioaccumulate and are environmentally persistent. Due to their serious health threats, including to humans, new methods for the sensing of PFAS are needed. Here, we report the electrochemical behaviour of perfluorooctanoic acid (PFOA) *via* ion transfer voltammetry at an array of microinterfaces between two immiscible electrolytic solutions (μITIES). Investigation of electrochemical sensing of PFOA at the μITIES array by voltammetry showed that differential pulse stripping voltammetry (DPSV) with a 300 s preconcentration time was the most sensitive approach. This enabled a limit of detection (LOD) of 1.2 nM. Matrix effects of different types of samples, like tap water, and aqueous phases spiked with a protein (bovine serum albumin) or complexing reagent (β-cyclodextrin), on the analytical performance of PFOA were evaluated. The findings presented here provide a basis for sensing of PFOA using ion transfer voltammetry.

Introduction

Per- and polyfluoroalkyl substances (PFAS) are synthetic pollutants that are highly persistent in the environment.[1–3] They have been widely used in firefighting foams, in paper and packaging industries, in clothing, in personal care products, in carpet manufacture as stain- and water-resistant coatings, and on various non-stick cookware.[1,2,4–8] PFAS are resistant to biodegradation, are distributed everywhere, and are persistent in the environment due to the strong fluorine-carbon bond.[9,10] Firefighting training sites,[11–15] landfill sites,[16,17] PFAS manufacturing sites,[14,18] and wastewater purification plants[14,19] are common zones of PFAS contamination. PFAS are also present in vegetables,[20,21] human breast milk[22,23] and blood serum,[24] and in drinking water.[14,25,26] Recently Whitehead *et al.* reported PFAS in various cosmetic products purchased in Canada and the United State of America (USA).[8]

PFAS can enter into living entities *via* contaminated drinking water, dust particles, foods (especially seafood), and various consumer items.[5,25,27–30] The lipophilic nature of PFAS causes bioaccumulation and toxicity.[31,32] The toxicity of PFAS to different aquatic (*e.g. Daphnia magna* and *Moina macrocopa*) and terrestrial (*e.g.* earthworm) species was investigated.[33,34] The toxicity of PFAS has been reported, for example DNA damage in earthworms[34] and *Escherichia coli*,[35] their effect on the neuroendocrine system of rats,[36] their effect on developmental toxicity and hepatotoxicity in monkeys[37] and their immunotoxicity in mice.[38] The toxicity and bioaccumulating nature of PFAS raise important environmental and human health concerns. PFAS has a negative effect in reproduction, immune function, endocrine function, and neurological function in humans.[32,39] Bartell and Vieira undertook a meta-analysis review of the role of one PFAS, perfluorooctanoic acid (PFOA), in kidney cancer and testicular cancer in humans, and suggested that the average cancer (kidney cancer and testicular cancer) risk is increased if the serum PFOA concentration is increased.[40] Since PFAS are directly implicated in toxic effects in different biological species, including humans, the availability of suitable methods for their analysis is important.

Methods based on liquid chromatography-tandem mass spectrometry (LC-MS/MS) and gas chromatography-mass spectrometry (GC-MS) are widely used for the determination of PFAS.[41–44] Even if the analytical performances of these techniques are suitable, common drawbacks include difficulty in on-site measurements, costs, instrumentation and sample pretreatment needs, and the requirement for highly-trained experts. Spectroscopic methods such as turn-on or turn-off fluorescence, and surface-enhanced Raman scattering are available for PFAS detection.[45–50] However, these still have some limitations like low selectivity, reasonable reproducibility, and the need for pretreatment steps.[50]

School of Molecular and Life Sciences, Curtin University, GPO Box U1987, Perth, Western Australia 6845, Australia. E-mail: d.arrigan@curtin.edu.au

† Electronic supplementary information (ESI) available. See DOI: https://doi.org/10.1039/d3sd00080j

Direct redox electrochemistry of PFAS is difficult to use for monitoring due to their high stability; despite this, electroanalytical approaches have received some attention.[51] For example, some researchers have detected PFAS by indirect redox electrochemistry using molecularly imprinted polymer (MIP) electrodes.[52–55] Karimian *et al.* (limit of detection (LOD) = 0.04 nM; *ca.* 20 ng L^{-1})[53] and Kazemi *et al.* (LOD = 0.05 nM; *ca.* 25 ng L^{-1})[55] reported MIP-modified electrochemical sensors for detection of perfluorooctane sulfonate (PFOS). Clark and Dick also detected PFOS (LOD = 3.4 pM; *ca.* 1.7 ng L^{-1}) present in river water using a MIP-modified carbon electrode.[52] Glasscott *et al.* reported a LOD of 250 fM (*ca.* 87 pg L^{-1}) for GenX using a MIP-modified microelectrode.[54] Ranaweera *et al.* used a bubble-nucleation approach on a nanoelectrode for the detection of PFOA and PFOS, yielding LODs of 72 nM (*ca.* 30 μg L^{-1}) and 160 nM (*ca.* 80 μg L^{-1}), respectively. This group also improved the LOD for PFOS to 0.08 nM (*ca.* 40 ng L^{-1}) by coupling with solid phase extraction.[56] Gong *et al.* developed a photoelectrochemical-based fluorescent sensor for the detection of PFOA, resulting in a LOD of 24 pM (*ca.* 0.01 μg L^{-1}).[57] Fang *et al.* also investigated PFOA detection using a MIP electrode, yielding a LOD of ~0.1 μM (*ca.* 41 μg L^{-1}).[58]

Similarly, electrochemistry at the interface between two immiscible electrolyte solutions (ITIES), which enables the non-redox detection of ionised or ionisable species, also opens a strategy for the detection of PFAS.[31] Ion transfer electrochemistry at the ITIES is used for detection of many ionisable analytes.[59] Problems with traditional electrochemical cells for measurements at the ITIES (*e.g.* mechanical instability, large capacitance) can be overcome by miniaturisation of the ITIES to the microscale.[60,61] This also has the added advantage of increasing mass transport flux to the ITIES.[62] Mechanical stability of the ITIES can be achieved by using a porous membrane or gelled organic phase.[63–65] Amemiya's group investigated the lipophilic nature of some PFAS at the ITIES[31] and also developed a method for the determination of PFAS using an organogel-based ITIES supported on a modified gold electrode; they reported a LOD of 50 pM (*ca.* 25 ng L^{-1}) for PFOS.[66] Viada *et al.* used a μITIES array to study PFOS and achieved a LOD of 30 pM (*ca.* 15 ng L^{-1}).[67] A recent study assessed the prospects for selectivity in the detection of PFAS mixtures by ion transfer electrochemistry at a micropipette-based μITIES.[68] Whilst PFOS can be detected sensitively at a μITIES array,[67] no studies were reported on PFOA detection at low concentrations.

The aim of the work reported here was to evaluate the electrochemical behaviour and detection of PFOA at a μITIES array. Different voltammetric techniques were employed, and the electroanalytical performances were assessed. Furthermore, matrix effects on the electrochemical response of PFOA were examined. The results show that PFOA sensing using electrochemistry at a μITIES array is viable approach.

Experimental section

Reagents

All reagents were purchased from Sigma-Aldrich Australia and used as received, unless otherwise indicated. Organic electrolyte salt bis(triphenylphosphoranylidene)ammonium tetrakis(4-chlorophenyl)borate (BTPPATPBCl) was synthesized by metathesis of equimolar quantities of bis(triphenylphosphoranylidene)ammonium chloride (BTPPACl) and potassium tetrakis(4-chlorophenyl)borate (KTPBCl) (STREM Chemicals).[69] The suitability of the prepared salt BTPPATPBCl was assessed by voltammograms in pure electrolyte solutions (*i.e.* no analyte present in either phase). The absence of peaks in these blank voltammograms indicated the absence of impurities and hence the suitability of the salt for these experiments. Pentadecafluorooctanoic acid (PFOA, purity: 98%) (STREM Chemicals) solutions were prepared in 10 mM lithium chloride (LiCl) solution unless otherwise indicated. Aqueous phase electrolyte solutions were LiCl (10 or 1 mM) or lithium sulfate (10 mM), and the organic phase electrolyte solution was 10 mM BTPPATPBCl or 10 mM tetradodecylammonum tetrakis(4-chlorophenyl) borate (TDDATPBCl) in 1,2-dichloroethane (1,2-DCE). All aqueous solutions were prepared using purified water with a resistivity of 18.2 MΩ cm (Milli-Q, Millipore Pty. Ltd., Australia). All experiments were conducted at ambient temperature.

Apparatus

Electrochemical measurements were conducted using an AUTOLAB PGSTAT302N electrochemical workstation (Metrohm, The Netherlands) controlled with the supplied NOVA software. These experiments were performed within a Faraday cage. All electrochemical measurements were performed using μITIES arrays prepared with glass membranes having 100 micropores (10 × 10 square array) made by laser ablation in a ~130 μm thick borosilicate substrate.[70] Due to the laser ablation process, the pores in the glass membranes were wider on the laser entry side (diameter: 42 μm) than on the laser exit side (diameter: 21 μm). One surface (laser exit side) of the glass membranes and the inner walls of the pores were made hydrophobic by silanisation with trichloro(1*H*,1*H*,2*H*,2*H*-perfluorooctyl)silane, while the other side (laser entry side) remained hydrophilic.[70] The glass membrane was sealed to the mouth of a glass cylinder using silicone sealant (Selley, Australia and New Zealand) such that the hydrophobic side faced towards the glass cylinder so the organic phase can be placed inside and subsequently into the pores. The sealant was allowed to cure for 24 h and the entire assembly was cleaned with acetone and dried in air before experiments. For each electrochemical cell set-up (Scheme 1), ~200 μL of organic electrolyte solution was placed into the glass cylinder. Then, the organic reference solution was placed on top of the organic phase (Scheme 1). By inserting this assembly into the aqueous phase and adding a pair of in-house prepared electrodes,

Ag | AgCl | 1 mM BTPPACl (10 mM LiCl)	10 mM BTPPATPBCl (1,2-DCE) (Org.)	10 mM LiCl + x μM PFOA (Aq.) | AgCl | Ag	Cell 1
Ag | AgCl | 1 mM TDDACl (10 mM LiCl)	10 mM TDDATPBCl (1,2-DCE) (Org.)	10 mM LiCl + x μM PFOA (Aq.) | AgCl | Ag	Cell 2
Ag | AgCl | 1 mM BTPPACl (10 mM LiCl)	10 mM BTPPATPBCl (1,2-DCE) (Org.)	10 mM Li_2SO_4 + x μM PFOA (Aq.) | Ag_2SO_4 | Ag	Cell 3
Ag | 1 mM BTPPACl (10 mM Li_2SO_4)	10 mM BTPPATPBCl (1,2-DCE) (Org.)	10 mM Li_2SO_4 + x μM PFOA (Aq.) | Ag	Cell 4
Ag | AgCl | 1 mM BTPPACl (10 mM LiCl)	10 mM BTPPATPBCl (1,2-DCE) (Org.)	1 mM LiCl + x μM PFOA (Aq.) | AgCl | Ag	Cell 5

Scheme 1 Schematic summary of electrochemical cell compositions used for the electrochemical study of PFOA. x = concentration of PFOA in the aqueous phase. Org. = organic phase and Aq. = aqueous phase.

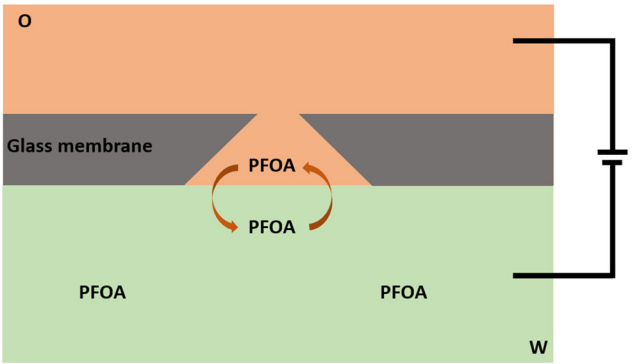

Fig. 1 Sketch representing the principle of ion transfer across the liquid–liquid interface using a μITIES array, illustrated here at a single conical-pore-based μITIES. O = organic phase; W = aqueous phase, containing PFOA. Arrows indicate movement of ionised PFOA between aqueous and organic phases under the influence of applied potential. Entire electrochemical cell compositions are presented in Scheme 1.

which were either silver/silver chloride, silver/silver sulfate or silver, a two-electrode cell was prepared. All electrochemical cells used during these experiments are summarised in Scheme 1. The pH of the aqueous phases was measured with a CP-511 Elmetron laboratory pH meter with combination pH electrode (Ionode, Queensland, Australia). This was calibrated with three pH buffer solutions (pH 4, 7, and 10) before measurements.

Electrochemical measurements

Cyclic voltammetry (CV), differential pulse voltammetry (DPV) and differential pulse stripping voltammetry (DPSV) were employed to study PFOA. The CV scan rate was 10 mV s^{-1}. The waveform parameters for DPV were: step potential: 0.005 V, modulation amplitude: 0.025 V, modulation time: 0.05 s, and interval time: 0.5 s. For each DPSV measurement, a 0.1 V preconcentration step (unless otherwise stated; time indicated in results) and a 0.5 V preconditioning potential (for 40 s) were applied.

Results and discussion

Cyclic voltammetry of PFOA

The electrochemical behaviour of PFOA at the μITIES array was investigated by CV in different electrochemical cell compositions (Scheme 1). Fig. 1 shows the principle of ion transfer electrochemical behaviour. Under the influence of an applied potential at the aqueous-organic interface, ionised PFOA will transfer and be detected. For CV, the transfer from water phase to organic phase occurs on the forward scan, and the back-transfer from organic to water phase occurs on the reverse scan. The study of different cell compositions was undertaken to understand the transfer behaviour of PFOA in the presence of different electrolyte concentrations and species, as these control the available potential window for voltammetric experiments. While chloride salts are usually used in the aqueous phase, and the transfer of chloride to the organic phase limits the negative side of the potential window at the ITIES, use of a sulfate salt in the aqueous phase might enable a wider potential window, due to its greater hydration energy, and hence might improve the ability to detect PFOA. Typical CVs are shown in Fig. 2. Asymmetric CVs were obtained in all cases, with steady-state voltammograms on the forward sweep (due to radial diffusion to the pores holding the μITIES), scanning from positive towards negative potentials, while the reverse-direction scans are peak shaped (due to linear diffusion within the pores), in agreement with previous studies.[67,68] CV also indicated no adsorption, emulsification, or instability of the interface.[67] In all cases, the reverse peak currents increased linearly with the PFOA concentration in the studied ranges (Fig. S1†). Similarly, calibration graph slope (sensitivity) of the current response to PFOA in the various cells and the LOD (defined as $3\sigma/m$, where σ is standard deviation of the blank (intercept) and m is the calibration graph slope) for PFOA in the various cells were also determined. Cell 1 displayed the greatest sensitivity (*ca.* 1.25 nA μM^{-1}) amongst these. Calculated sensitivity of cells 2, 3, and 4 were *ca.* 0.78, *ca.* 0.87, and *ca.* 0.85 nA μM^{-1}, respectively. Also, cells 3 (LOD = 0.3 μM) and 4 (LOD = 1.1 μM) gave lower LODs than cells 1 (LOD = 3.5 μM) and 2 (LOD = 2.3 μM). The lower LODs of cells 3, 4 are due to the presence of more hydrophilic aqueous supporting electrolyte anion, *i.e.* SO_4^{2-}, which produced a wider potential window compared to cells with Cl^- (which is less hydrophilic than SO_4^{2-}) as the aqueous phase electrolyte anion. The LODs found in all cells show that CV is not sufficient for the detection of the lower concentrations of PFOA required for most applications. Although the sensitivities and LODs in SO_4^{2-}-based electrolytes are slightly lower, Cl^--based electrolytes were selected for further studies because of the presence of Cl^- in most environmental or biological samples.

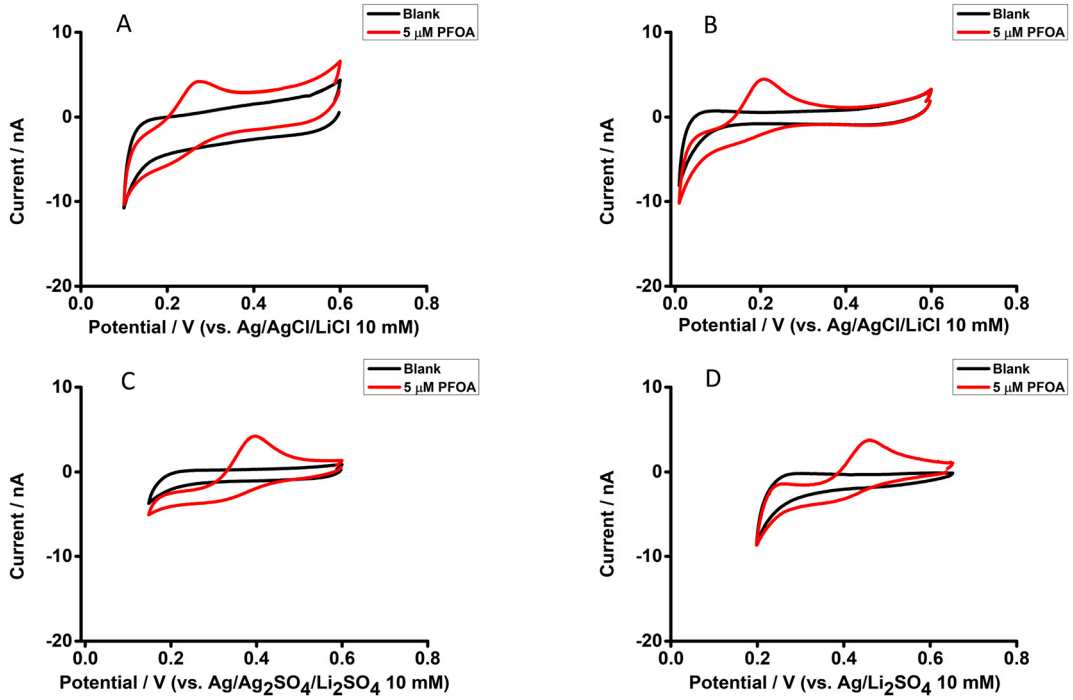

Fig. 2 CVs without background-subtraction in the presence and absence (black) of PFOA in the aqueous phase. (A) 10 mM LiCl as the aqueous phase (pH = 6.0) and 10 mM BTPPATPBCl (1,2-DCE) as the organic phase using cell 1. (B) 10 mM LiCl as the aqueous phase (pH = 6.0) and 10 mM TDDATPBCl as the organic phase using cell 2. (C) and (D) 10 mM Li_2SO_4 as the aqueous phase (pH = 6.3) and 10 mM BTPPATPBCl (1,2-DCE) as the organic phase using cell 3 and cell 4, respectively. Scan rate: 10 mV s^{-1}.

Influence of pH on the electrochemical behaviour of PFOA

The electrochemical behaviour of PFOA at different aqueous phase pH values was explored using cell 1 (Scheme 1). Fig. 3 shows CVs of 10 μM PFOA at different aqueous phase pH. As can be seen, an indistinct reverse peak current was seen at pH ≤ 3; however, distinct current signals were observed at higher pH. Since the pK_α of PFOA is 2.8,[71] the lower peak current and poor shape of the voltammogram at lower pH is due to incomplete dissociation of PFOA and hence less anionic PFOA is available to transfer. Similarly, the higher peak current at pH ≥ 4 is due to availability of more anionic PFOA for transfer due to complete dissociation of PFOA. This is also supported by the fit of experimental data to the theoretical relationship between the pH and fraction of anionic PFOA (inset, Fig. 3). These results demonstrate that pH ≥ 4 is best for the electrochemical study of PFOA at the ITIES.

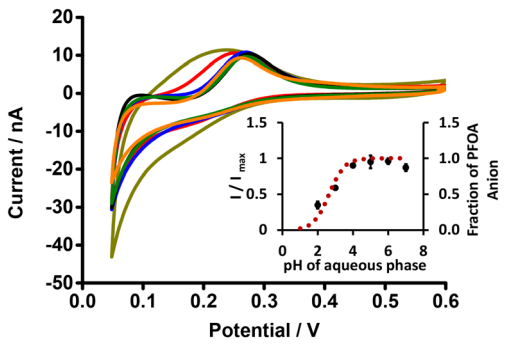

Fig. 3 CVs of PFOA at different pH of aqueous phase (dark yellow, red, blue, black, olive, and orange lines respectively indicate CVs at pH 2, 3, 4, 5, 6, and 7) (without background-subtraction). 10 mM BTPPATPBCl (1,2-DCE) as the organic phase. Inset: Plot of I/I_{max} (black dots) or fraction of PFOA anion (red dotted line) *versus* pH of the aqueous phase. Concentration of PFOA: 10 μM, scan rate: 10 mV s^{-1}. Error bars represent ±1 standard deviation from three independent experiments.

Differential pulse voltammetry of PFOA

The μITIES array was used to conduct DPV, which is well-known[72] to achieve the detection of lower concentrations of the analyte compared to CV. Background-subtracted followed by baseline-corrected DPVs at different concentrations are presented in Fig. 4(A and B) using cell 1. Calibration curves between peak current and concentration of PFOA for all DPVs indicate that the peak current linearly increased with PFOA concentration. Five electrochemical cell compositions, including cell 1, were used for the DPV detection of PFOA (voltammograms are shown in Fig. S2† for cells 2, 3, 4 and 5).

Table 1 summarises the DPV analytical characteristics for PFOA. Higher sensitivities and lower LODs were obtained in the backward-scan direction compared to the forward-scan direction using cell 1. Amongst all cells, the highest sensitivity was found in cell 2 (Table 1), the lowest LOD (0.01 μM) was found in cell 5, while the highest LOD (0.12 μM) was found in cell 3. LODs from DPV were lower than those from CV, as expected. As described in the literature, further

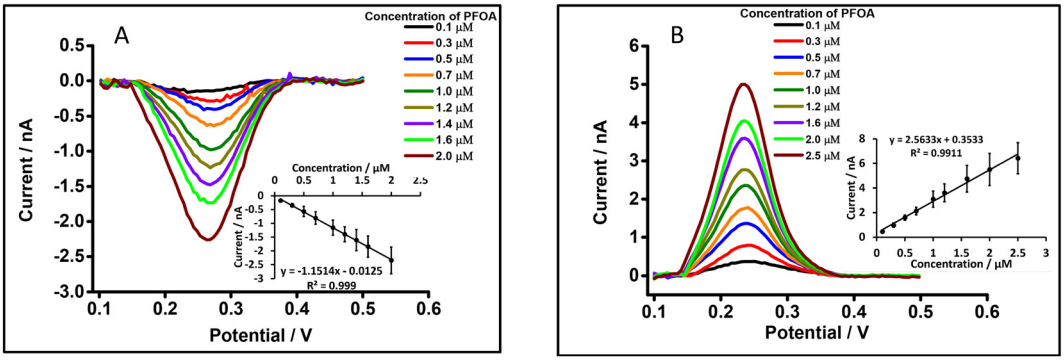

Fig. 4 DPVs at different concentrations of PFOA at the μITIES array using cell 1. (A) and (B) represent DPVs for forward and backward scan, respectively, using 10 mM LiCl as the aqueous phase (pH = 6.0) and 10 mM BTPPATPBCl (1,2-DCE) as the organic phase. Insets: Calibration curves between current and concentration of PFOA. Error bars represent ±1 standard deviation from three different independent measurements. All DPVs were background-subtracted then baseline-corrected.

lowering of LODs could be achieved by the application of a systematic preconcentration step.[73–75] Since the detection capability of PFOA using cell 5 (Scheme 1) was the best, this cell composition was used for further improvement of the LOD for PFOA by stripping voltammetry.

Differential pulse stripping voltammetry of PFOA

DPSV combines the advantages of an inherent preconcentration of the analyte with detection by differential pulse voltammetry,[76] and so offers the prospect for improved analyte detection relative to DPV and CV. In DPSV, a preconcentration step at a fixed potential is followed by a voltammetric scan, providing the two steps involved in this analytical approach. LODs are improved by choosing an appropriate preconcentration step. Based on the CV behaviour (Fig. S3†), 0.1 V was chosen as the preconcentration potential. At this potential, ionised PFOA is driven from the aqueous phase into the organic phase where it is accumulated. Additionally, the geometry of the pores in the membrane used to form the μITIES array (Fig. 1) also affects the accumulation of PFOA in this analytical strategy. If the pores of the membrane are tapered towards the organic phase side, diffusion of PFOA through the pores into the bulk organic phase is restricted, and hence the concentration of PFOA in the organic phase within the pores is enhanced.[70] At the end of the preconcentration period, DPV is applied as the detection step to strip the accumulated PFOA from the organic phase back to the aqueous phase and produce a peak response that is dependent on both PFOA concentration and the preconcentration time.

Table 1 Comparison of sensitivity and limit of detection for PFOA using DPV in different electrochemical cells

Cell used	Scan direction	Calibration graph slope/nA μM^{-1}	LOD/μM
Cell 1	Forward	1.2	0.06
Cell 1	Backward	2.6	0.05
Cell 2	Backward	4.0	0.05
Cell 3	Backward	2.1	0.12
Cell 4	Backward	2.2	0.09
Cell 5	Backward	2.9	0.01

Effect of preconcentration time in detection of PFOA using DPSV

Preconcentration time is an important parameter in the detection of analytes by DPSV. Here, based on the DPV results, cell 5 (Scheme 1) was used to study the effects of preconcentration time (at 0.5 μM PFOA), without stirring of the aqueous phase, because mass transport by radial diffusion is achieved by use of a μITIES array. Fig. 5 shows DPSVs of PFOA at different preconcentration times. The results show that the peak response increased with preconcentration time and reached a plateau after 200 s (inset, Fig. 5). The plateau indicates a saturation effect, as described for a range of other analytes.[67,75,77–79] Therefore, a

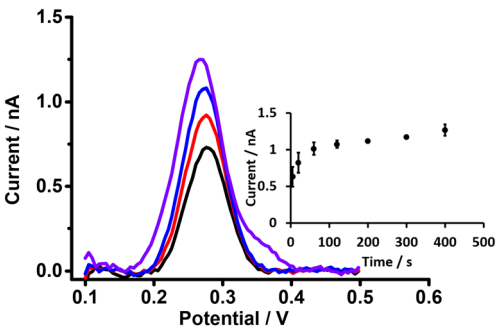

Fig. 5 DPSVs of 0.5 μM of PFOA at different preconcentration times using the μITIES array with cell 5. 10 mM BTPPATPBCl (1,2-DCE) as the organic phase. Black, red, blue, and violet lines respectively indicate CVs at 5, 20, 60, and 400 s, respectively. 1 mM LiCl as the aqueous phase (pH = 6.4), unstirred. Preconcentration times: 5–400 s. Inset: calibration curve between stripping peak currents and preconcentration times. Error bars are ±1 standard deviation obtained from three different experimental trials. All DPSVs were background-subtracted followed by baseline-corrected.

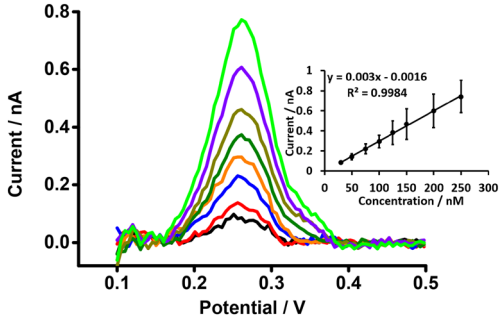

Fig. 6 DPSVs at different concentrations of PFOA at a μITIES array using cell 5. Organic phase: 10 mM BTPPATPBCl (1,2-DCE). 1 mM LiCl as the aqueous phase (pH = 6.4), concentration range (30–250 nM). Black, red, blue, orange, olive, dark yellow, violet and green lines respectively indicate CVs at 30, 50, 75, 100, 125, 150, 200, and 250 nM, respectively. Inset: calibration curve between stripping current and concentration of PFOA. Data points are average of three different trials, and error bars are ±1 standard deviation. All DPSVs were background-subtracted followed by baseline-corrected.

preconcentration time of 300 s was chosen as suitable for the further investigation of PFOA detection by DPSV.

Detection of PFOA using DPSV

DPSV at the μITIES array was further tested to detect PFOA at lower concentrations using cell 5 (Scheme 1) with a 300 s preconcentration time. The results show that the stripping peak current was concentration-dependent in the range 30–250 nM (Fig. 6). Linear behaviour was obtained (inset, Fig. 6), yielding LOD ($3\sigma/m$) and sensitivity values of 1.2 nM (0.5 μg L^{-1}) and 0.003 nA nM^{-1}, respectively. However, Viada *et al.* achieved a picomolar LOD for PFOS using a μITIES array with DPSV and a 300 s preconcentration time.[67] Since the carboxylate group in PFOA possesses stronger hydration than the sulfonate of PFOS, PFOA has lower lipophilicity than PFOS.[66,80] As reported in the literature, the preconcentration step is more favourable for more lipophilic species, like PFOS.[81] As a result, the higher LOD for PFOA compared to PFOS might be due to its lower lipophilicity. Many other investigations also detected lower concentrations of PFOS than PFOA.[82–84] Nevertheless, the LOD obtained here for PFOA is the lowest obtained for ion-transfer stripping voltammetry of PFOA at the μITIES array and shows that this detection approach was better than those of Ranaweera *et al.*, using a Pt nanoelectrode (LOD = 72 nM; 30 μg L^{-1}),[56] Cheng *et al.*, using a fluorescent sensor for the detection of PFOA (LOD = 11.8 nM; *ca.* 5 μg L^{-1}),[45] Shanbhag *et al.*, using hafnium-doped tungsten oxide as electrode material (LOD = 18.3 nM (7.6 μg L^{-1}),[85] Fang *et al.*, using a MIP electrode (LOD = ~100 nM; *ca.* 41 μg L^{-1}),[58] and Sahu *et al.*, using screen-printed electrodes (LOD = 15 nM; 6.5 μg L^{-1}).[86] Table S1† compares the analytical performances for PFOA with these different analytical approaches. However, many chromatographic-mass spectrometric approaches (*e.g.* HPLC-MS, GC-MS, and LC-MS-MS) are widely used for the detection of PFAS, and these can detect picomolar or even lower concentrations, showing lower LODs than our approach. But these methods have several drawbacks (*e.g.* need for expert users, time consuming, sample preparation step, expense, difficulty in on-site measurement).[50,87–89] The LOD achieved here is comparable to the recommended limit of 1.4 nM (*ca.* 0.56 μg L^{-1}) for drinkable water set by the Department of Health, Australia,[90] but significantly higher than the level established by the USA Environmental Protection Agency (EPA) (10 fM; *ca.* 0.004 ng L^{-1}).[91] Nevertheless, the analytical capability is lower than the recommended level of 24 nM (*ca.* 10 μg L^{-1}) for recreational waters (Department of Health, Australia),[90] suggesting that it could potentially be used to pre-screen environmental samples for PFOA contamination, with potential benefits in both time and money terms.

Study of matrix effects on electrochemical response of PFOA

For appropriate monitoring of the concentration of PFAS pollutants, knowledge of any matrix effects is important because the matrix components might alter the electrochemical signal of the analyte.[92–94] These impacts may be due to one or more of the following reasons: a) interaction between the analyte and other components of a sample which sequester the analyte making it unavailable for detection, b) interaction of matrix components with the sensing interface, which makes it more difficult to sense the analyte, and c) overlap of transfer potential of matrix components and the analyte of interest. Accordingly, for the development of a PFOA sensor, a matrix effect study is very important.

Matrix effect of different types of water

Different water types were analysed to see if there was a matrix effect on the PFOA response. Fig. 7A and B show background-subtracted followed by baseline corrected DPVs of PFOA using drinking water (with 10 mM LiCl) and laboratory tap water (with 10 mM LiCl) (water taken from local supplies at Curtin University), respectively, as the aqueous phase. For comparison, Fig. 7C and D show the corresponding water samples without added 10 mM LiCl. These results show that there is a slight shift in the peak potential of PFOA depending on whether added 10 mM LiCl is present, which is attributed to differences in chloride composition of the water and the dependence of the aqueous phase reference electrode on this chloride content.[95] Likewise, the peak responses of PFOA in both matrices were slightly decreased compared to the aqueous phase comprised of 10 mM LiCl in high purity water (Fig. 4B). However, in simple matrices like clean water, there is little impact of the sample matrix on the detection capability.

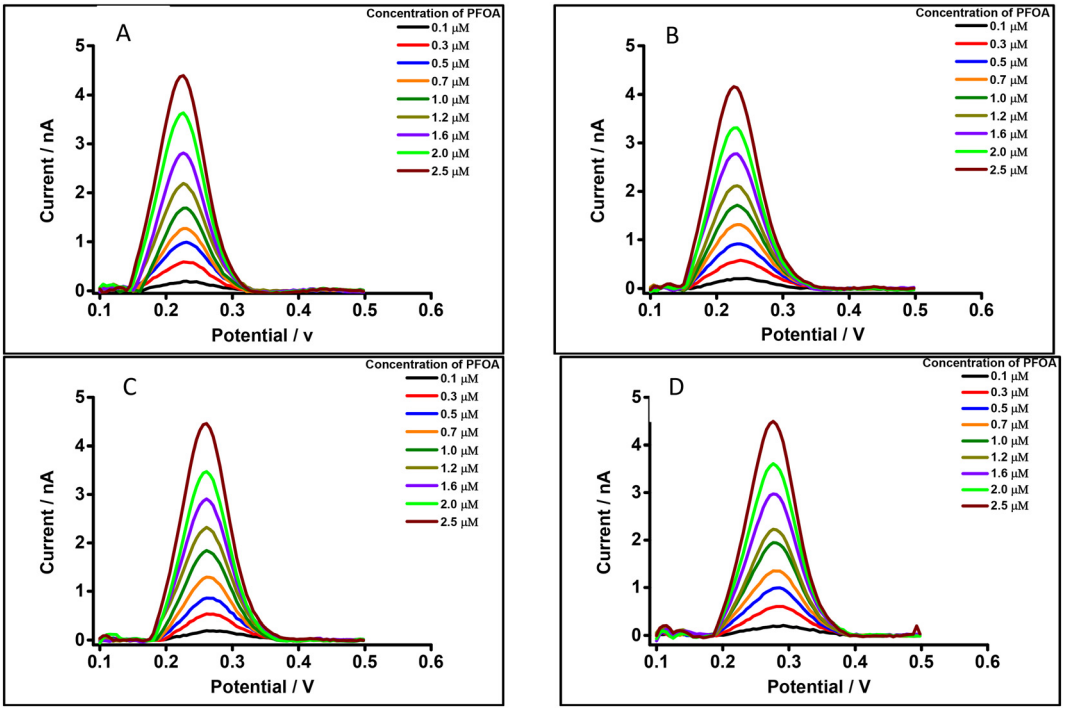

Fig. 7 DPVs of PFOA using 10 mM BTPPATPBCl (1,2-DCE) as the organic phase, cell 1. Concentration range: 0.1–2.5 μM. (A) Drinking water with 10 mM LiCl as the aqueous phase (pH = 7.4), (B) laboratory tap water with 10 mM LiCl as the aqueous phase (pH = 7.2), (C) drinking water without LiCl as the aqueous phase (pH = 7.4), (D) laboratory tap water without LiCl as the aqueous phase (pH = 7.2). All DPVs were background-subtracted followed by baseline corrected.

Matrix effects of bovine serum albumin (BSA) and β-cyclodextrin (β-CD)

Studies have shown that PFAS such as PFOA and PFOS interact with serum albumin to form complexes.[96,97] Likewise, β-CD forms a complex with PFAS, *e.g.* PFOA.[98,99] In order to understand possible matrix effects of BSA and β-CD on the detection of PFOA at a μITIES array, experiments were undertaken using DPV in the presence of a physiological concentration of BSA (*i.e.* 42 mg mL^{-1}; *ca.* 0.6 mM)[100] in 10 mM LiCl as the aqueous phase. Fig. 8A displays DPVs of different concentrations of PFOA in the presence of this concentration of BSA. The results reveal that the detection of PFOA in the presence of the physiological concentration of BSA is significantly attenuated compared to without BSA (Fig. 4B). However, once PFOA was detected, the DPV current increased linearly with PFOA concentration. Similarly, the effect of β-CD on the electrochemical response of PFOA was also investigated, in the presence of 0.6 mM β-CD in 10 mM LiCl aqueous phase. Fig. 8B shows DPVs of different concentrations of PFOA at fixed concentration of β-CD. At higher PFOA concentrations, there is linearity between the peak current and PFOA concentration. In the presence of β-CD, detection of PFOA is easier than in the presence of the

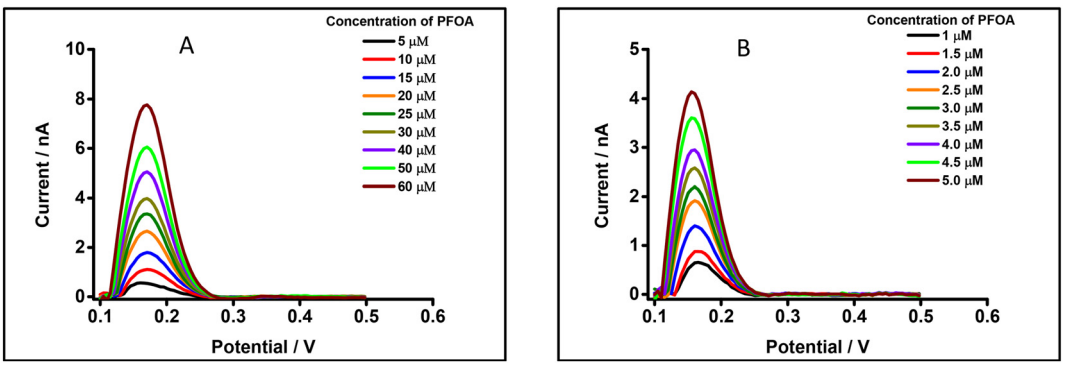

Fig. 8 DPVs of PFOA using 10 mM BTPPATPBCl (1,2-DCE) as the organic phase. (A) 0.6 mM BSA in 10 mM LiCl as the aqueous phase (pH = 6.8). Concentration range: 5–60 μM of PFOA. (B) 0.6 mM β-CD in 10 mM LiCl as the aqueous phase (pH = 7.3). Concentration range: 1–5 μM of PFOA. All DPVs were background-subtracted followed by baseline corrected.

same concentration of BSA. However, the detection of PFOA in the presence of 0.6 mM β-CD is lower than in absence of β-CD (Fig. 4B). These results show that BSA or β-CD have a significant influence on the electrochemical response of PFOA. This is attributed to the complexation of PFOA by BSA or by β-CD; this complexation removes free ionised PFOA from solution and makes it unavailable for transfer across the ITIES. BSA and β-CD are used here as model complexants for PFOA, illustrating the possible impact of matrix components that sequester PFOA in samples and consequently alter the detection sensitivity.

Conclusions

PFOA is an anthropogenic environmental contaminant which is persistent and bioaccumulative in nature. In this study, the electrochemical behaviour of PFOA and the sensitivity of different voltammetric techniques for the detection of PFOA at the μITIES array were investigated. CV revealed that steady state current and peak current were obtained, respectively, for water to organic and organic to water transfers. A pH study revealed that the pH of the aqueous phase pH $\leq$ 3 is unsuitable for the detection of PFOA, due to its acid–base properties. Among the techniques studied, DPSV was the most sensitive. The lowest LOD for PFOA was 1.2 nM (0.5 μg L^{-1}), following preconcentration at 0.1 V for 300 s without stirring. Furthermore, the matrix study revealed that the electrochemical response of PFOA was impacted by the matrix component of the studied sample. Overall these results show that PFOA electrochemistry at the μITIES array may be useful for screening and detection of PFOA in environmental samples.

Conflicts of interest

There are no conflicts of interest to declare.

Acknowledgements

We thank Curtin University for provision of a PhD Scholarship to HBL. We thank the South Australian and OptoFab nodes of the NCRIS-enabled Australian National Fabrication Facility (ANFF-SA and ANFF-OptoFab, respectively) for fabrication of the glass microporous membranes.

References

1 R. C. Buck, J. Franklin, U. Berger, J. M. Conder, I. T. Cousins, P. de Voogt, A. A. Jensen, K. Kannan, S. A. Mabury and S. P. J. van Leeuwen, *Integr. Environ. Assess. Manage.*, 2011, **7**, 513–541.

2 A. Falk-Filipsson, S. Fischer, J. Ivarsson, J. Forsberg and M. Delvin, *Occurrence and use of highly fluorinated substances and alternatives*, The Swedish Chemical Agency (KEMI), Stockholm, 2015.

3 E. Kissa, *Fluorinated Surfactants and Repellents*, Marcel Dekker, New York, 2001.

4 G. W. Curtzwiler, P. Silva, A. Hall, A. Ivey and K. Vorst, *Integr. Environ. Assess. Manage.*, 2021, **17**, 7–12.

5 J. R. Lang, B. M. Allred, G. F. Peaslee, J. A. Field and M. A. Barlaz, *Environ. Sci. Technol.*, 2016, **50**, 5024–5032.

6 X. Trier, K. Granby and J. H. Christensen, *Environ. Sci. Pollut. Res.*, 2011, **18**, 1108–1120.

7 J. Glüge, M. Scheringer, I. T. Cousins, J. C. DeWitt, G. Goldenman, D. Herzke, R. Lohmann, C. A. Ng, X. Trier and Z. Wang, *Environ. Sci.: Processes Impacts*, 2020, **22**, 2345–2373.

8 H. D. Whitehead, M. Venier, Y. Wu, E. Eastman, S. Urbanik, M. L. Diamond, A. Shalin, H. Schwartz-Narbonne, T. A. Bruton, A. Blum, Z. Wang, M. Green, M. Tighe, J. T. Wilkinson, S. McGuinness and G. F. Peaslee, *Environ. Sci. Technol. Lett.*, 2021, **8**, 538–544.

9 M. F. Rahman, S. Peldszus and W. B. Anderson, *Water Res.*, 2014, **50**, 318–340.

10 N. A. Fernandez, L. Rodriguez-Freire, M. Keswani and R. Sierra-Alvarez, *Environ. Sci.: Water Res. Technol.*, 2016, **2**, 975–983.

11 J. L. Guelfo and D. T. Adamson, *Environ. Pollut.*, 2018, **236**, 505–513.

12 S. Banzhaf, M. Filipovic, J. Lewis, C. J. Sparrenbom and R. Barthel, *Ambio*, 2017, **46**, 335–346.

13 X. Dauchy, V. Boiteux, C. Bach, C. Rosin and J. F. Munoz, *Chemosphere*, 2017, **183**, 53–61.

14 X. C. Hu, D. Q. Andrews, A. B. Lindstrom, T. A. Bruton, L. A. Schaider, P. Grandjean, R. Lohmann, C. C. Carignan, A. Blum, S. A. Balan, C. P. Higgins and E. M. Sunderland, *Environ. Sci. Technol. Lett.*, 2016, **3**, 344–350.

15 V. Boiteux, C. Bach, V. Sagres, J. Hemard, A. Colin, C. Rosin, J. F. Munoz and X. Dauchy, *Int. J. Environ. Anal. Chem.*, 2016, **96**, 705–728.

16 H. Yan, I. T. Cousins, C. Zhang and Q. Zhou, *Sci. Total Environ.*, 2015, **524–525**, 23–31.

17 C. Gallen, D. Drage, G. Eaglesham, S. Grant, M. Bowman and J. F. Mueller, *J. Hazard. Mater.*, 2017, **331**, 132–141.

18 C. Bach, X. Dauchy, V. Boiteux, A. Colin, J. Hemard, V. Sagres, C. Rosin and J.-F. Munoz, *Environ. Sci. Pollut. Res.*, 2017, **24**, 4916–4925.

19 T. L. Coggan, D. Moodie, A. Kolobaric, D. Szabo, J. Shimeta, N. D. Crosbie, E. Lee, M. Fernandes and B. O. Clarke, *Heliyon*, 2019, **5**, e02316.

20 M. S. Lal, M. Megharaj, R. Naidu and M. M. Bahar, *Environ. Technol. Innovation*, 2020, **19**, 100863.

21 J. Bao, C. L. Li, Y. Liu, X. Wang, W. J. Yu, Z. Q. Liu, L. X. Shao and Y. H. Jin, *Environ. Res.*, 2020, **188**, 109751.

22 M. K. So, N. Yamashita, S. Taniyasu, Q. Jiang, J. P. Giesy, K. Chen and P. K. S. Lam, *Environ. Sci. Technol.*, 2006, **40**, 2924–2929.

23 G. Zheng, E. Schreder, J. C. Dempsey, N. Uding, V. Chu, G. Andres, S. Sathyanarayana and A. Salamova, *Environ. Sci. Technol.*, 2021, **55**, 7510–7520.

24 L. M. L. Toms, A. M. Calafat, K. Kato, J. Thompson, F. Harden, P. Hobson, A. Sjödin and J. F. Mueller, *Environ. Sci. Technol.*, 2009, **43**, 4194–4199.

25 J. Thompson, G. Eaglesham and J. Mueller, *Chemosphere*, 2011, **83**, 1320–1325.
26 O. Quiñones and S. A. Snyder, *Environ. Sci. Technol.*, 2009, **43**, 9089–9095.
27 S. Hansen, R. Vestergren, D. Herzke, M. Melhus, A. Evenset, L. Hanssen, M. Brustad and T. M. Sandanger, *Environ. Int.*, 2016, **94**, 272–282.
28 P. A. Fair, B. Wolf, N. D. White, S. A. Arnott, K. Kannan, R. Karthikraj and J. E. Vena, *Environ. Res.*, 2019, **171**, 266–277.
29 F. Xiao, *Water Res.*, 2017, **124**, 482–495.
30 C. Tang, J. Tan, C. Wang and X. Peng, *J. Chromatogr. A*, 2014, **1341**, 50–56.
31 P. Jing, P. J. Rodgers and S. Amemiya, *J. Am. Chem. Soc.*, 2009, **131**, 2290–2296.
32 L. J. L. Espartero, M. Yamada, J. Ford, G. Owens, T. Prow and A. Juhasz, *Environ. Res.*, 2022, **212**, 113431.
33 K. Ji, Y. Kim, S. Oh, B. Ahn, H. Jo and K. Choi, *Environ. Toxicol. Chem.*, 2008, **27**, 2159–2168.
34 D. Xu, C. Li, Y. Wen and W. Liu, *Environ. Pollut.*, 2013, **174**, 121–127.
35 G. Liu, S. Zhang, K. Yang, L. Zhu and D. Lin, *Environ. Pollut.*, 2016, **214**, 806–815.
36 M. E. Austin, B. S. Kasturi, M. Barber, K. Kannan, P. S. MohanKumar and S. M. J. MohanKumar, *Environ. Health Perspect.*, 2003, **111**, 1485–1489.
37 A. M. Seacat, P. J. Thomford, K. J. Hansen, G. W. Olsen, M. T. Case and J. L. Butenhoff, *Toxicol. Sci.*, 2002, **68**, 249–264.
38 Q. Yang, M. Abedi-Valugerdi, Y. Xie, X. Y. Zhao, G. Möller, B. D. Nelson and J. W. DePierre, *Int. Immunopharmacol.*, 2002, **2**, 389–397.
39 M. Kirk, K. Smurthwaite, J. Bräunig, S. Trevenar, C. D'Este, R. Lucas, A. Lal, R. Korda, A. Clements, J. Mueller and B. P. Armstrong, *The PFAS Health Study: Systematic Literature Review*, The Australian National University, Canberra, 2018.
40 S. M. Bartell and V. M. Vieira, *J. Air Waste Manage. Assoc.*, 2021, **71**, 663–679.
41 M. Trojanowicz and M. Koc, *Microchim. Acta*, 2013, **180**, 957–971.
42 M. Takino, S. Daishima and T. Nakahara, *Rapid Commun. Mass Spectrom.*, 2003, **17**, 383–390.
43 S. Poothong, S. K. Boontanon and N. Boontanon, *J. Hazard. Mater.*, 2012, **205–206**, 139–143.
44 C. Gremmel, T. Frömel and T. P. Knepper, *Anal. Bioanal. Chem.*, 2017, **409**, 1643–1655.
45 Z. Cheng, L. Du, P. Zhu, Q. Chen and K. Tan, *Spectrochim. Acta, Part A*, 2018, **201**, 281–287.
46 Z. Cheng, H. Dong, J. Liang, F. Zhang, X. Chen, L. Du and K. Tan, *Spectrochim. Acta, Part A*, 2019, **207**, 262–269.
47 Y. Wang and H. Zhu, *Anal. Methods*, 2014, **6**, 2379–2383.
48 Q. Liu, A. Huang, N. Wang, G. Zheng and L. Zhu, *J. Lumin.*, 2015, **161**, 374–381.
49 C. Fang, M. Megharaj and R. Naidu, *RSC Adv.*, 2016, **6**, 11140–11145.
50 H. Ryu, B. Li, S. De Guise, J. McCutcheon and Y. Lei, *J. Hazard. Mater.*, 2021, **408**, 124437.
51 H. B. Lamichhane and D. W. M. Arrigan, *Curr. Opin. Electrochem.*, 2023, **40**, 101309.
52 R. B. Clark and J. E. Dick, *ACS Sens.*, 2020, **5**, 3591–3598.
53 N. Karimian, A. M. Stortini, L. M. Moretto, C. Costantino, S. Bogialli and P. Ugo, *ACS Sens.*, 2018, **3**, 1291–1298.
54 M. W. Glasscott, K. J. Vannoy, R. Kazemi, M. D. Verber and J. E. Dick, *Environ. Sci. Technol. Lett.*, 2020, **7**, 489–495.
55 R. Kazemi, E. I. Potts and J. E. Dick, *Anal. Chem.*, 2020, **92**, 10597–10605.
56 R. Ranaweera, C. Ghafari and L. Luo, *Anal. Chem.*, 2019, **91**, 7744–7748.
57 J. Gong, T. Fang, D. Peng, A. Li and L. Zhang, *Biosens. Bioelectron.*, 2015, **73**, 256–263.
58 C. Fang, Z. Chen, M. Megharaj and R. Naidu, *Environ. Technol. Innovation*, 2016, **5**, 52–59.
59 P. Vanýsek and L. B. Ramírez, *J. Chil. Chem. Soc.*, 2008, **53**, 1455–1463.
60 A. A. Stewart, G. Taylor, H. H. Girault and J. McAleer, *J. Electroanal. Chem. Interfacial Electrochem.*, 1990, **296**, 491–515.
61 G. Taylor and H. H. J. Girault, *J. Electroanal. Chem. Interfacial Electrochem.*, 1986, **208**, 179–183.
62 M. D. Scanlon and D. W. M. Arrigan, *Electroanalysis*, 2011, **23**, 1023–1028.
63 G. Herzog, *Analyst*, 2015, **140**, 3888–3896.
64 T. Kakutani, T. Ohkouchi, T. Osakai, T. Kakiuchi and M. Senda, *Anal. Sci.*, 1985, **1**, 219–225.
65 T. Osakai, T. Kakutani and M. Senda, *Bunseki Kagaku*, 1984, **33**, E371–E377.
66 M. B. Garada, B. Kabagambe, Y. Kim and S. Amemiya, *Anal. Chem.*, 2014, **86**, 11230–11237.
67 B. N. Viada, L. M. Yudi and D. W. M. Arrigan, *Analyst*, 2020, **145**, 5776–5786.
68 G. J. Islam and D. W. M. Arrigan, *ACS Sens.*, 2022, **7**, 2960–2967.
69 A. J. Olaya, M. A. Méndez, F. Cortes-Salazar and H. H. Girault, *J. Electroanal. Chem.*, 2010, **644**, 60–66.
70 E. Alvarez de Eulate, J. Strutwolf, Y. Liu, K. O'Donnell and D. W. M. Arrigan, *Anal. Chem.*, 2016, **88**, 2596–2604.
71 N. O. Brace, *J. Org. Chem.*, 1962, **27**, 4491–4498.
72 A. J. Bard, L. R. Faulkner and H. S. White, *Electrochemical Methods: Fundamentals and Applications*, John Wiley & Sons, 2022, p. 369.
73 M. M. Hossain, S. H. Lee, H. H. Girault, V. Devaud and H. J. Lee, *Electrochim. Acta*, 2012, **82**, 12–18.
74 H. R. Kim, C. M. Pereira, H. Y. Han and H. J. Lee, *Anal. Chem.*, 2015, **87**, 5356–5362.
75 G. Herzog and V. Beni, *Anal. Chim. Acta*, 2013, **769**, 10–21.
76 C. Ariño, C. E. Banks, A. Bobrowski, R. D. Crapnell, A. Economou, A. Krolicka, C. Perez-Rafols, D. Soulis and J. Wang, *Nat. Rev. Methods Primers*, 2022, **2**, 62.
77 J. Strutwolf, M. D. Scanlon and D. W. M. Arrigan, *J. Electroanal. Chem.*, 2010, **641**, 7–13.
78 M. D. Scanlon, G. Herzog and D. W. M. Arrigan, *Anal. Chem.*, 2008, **80**, 5743–5749.

79 X. Jiang, K. Gao, D. Hu, H. Wang, S. Bian and Y. Chen, *Analyst*, 2015, **140**, 2823–2833.
80 S. Kihara, M. Suzuki, M. Sugiyama and M. Matsui, *J. Electroanal. Chem. Interfacial Electrochem.*, 1988, **249**, 109–122.
81 Y. Kim, P. J. Rodgers, R. Ishimatsu and S. Amemiya, *Anal. Chem.*, 2009, **81**, 7262–7270.
82 L. D. Chen, C. Z. Lai, L. P. Granda, M. A. Fierke, D. Mandal, A. Stein, J. A. Gladysz and P. Bühlmann, *Anal. Chem.*, 2013, **85**, 7471–7477.
83 Z. Zheng, H. Yu, W. C. Geng, X. Y. Hu, Y. Y. Wang, Z. Li, Y. Wang and D. S. Guo, *Nat. Commun.*, 2019, **10**, 5762.
84 J. Wang, Y. Shi and Y. Cai, *J. Chromatogr. A*, 2018, **1544**, 1–7.
85 M. M. Shanbhag, N. P. Shetti, S. S. Kalanur, B. G. Pollet, M. N. Nadagouda and T. M. Aminabhavi, *Chem. Eng. J.*, 2022, **434**, 134700.
86 S. P. Sahu, S. Kole, C. G. Arges and M. R. Gartia, *ACS Omega*, 2022, **7**, 5001–5007.
87 R. F. Menger, E. Funk, C. S. Henry and T. Borch, *Chem. Eng. J.*, 2021, **417**, 129133.
88 C. A. Huset and K. M. Barry, *MethodsX*, 2018, **5**, 697–704.
89 K. L. Rodriguez, J. H. Hwang, A. R. Esfahani, A. H. M. A. Sadmani and W. H. Lee, *Micromachines*, 2020, **11**, 667.
90 Department of Health, Health Based Guidance values for Per- and Poly-fluoroalkyl substances (PFAS), **https://www.health.gov.au/sites/default/files/documents/2022/07/health-based-guidance-values-for-pfas-for-use-in-site-investigations-in-australia_0.pdf**, (accessed 05/March/2023).
91 Drinking Water Health Advisories for PFOA and PFOS, 2022 Interim Updated PFOA and PFOS Health Advisories, **https://www.epa.gov/sdwa/drinking-water-health-advisories-pfoa-and-pfos**, (accessed 01/January/2023).
92 Y. Liu, J. Bao, X. M. Hu, G. L. Lu, W. J. Yu and Z. H. Meng, *Microchem. J.*, 2020, **155**, 104673.
93 J. Cheng, C. D. Vecitis, H. Park, B. T. Mader and M. R. Hoffmann, *Environ. Sci. Technol.*, 2008, **42**, 8057–8063.
94 C. E. Schaefer, C. Andaya, A. Burant, C. W. Condee, A. Urtiaga, T. J. Strathmann and C. P. Higgins, *Chem. Eng. J.*, 2017, **317**, 424–432.
95 K. R. Temsamani and K. L. Cheng, *Sens. Actuators, B*, 2001, **76**, 551–555.
96 X. Han, T. A. Snow, R. A. Kemper and G. W. Jepson, *Chem. Res. Toxicol.*, 2003, **16**, 775–781.
97 P. D. Jones, W. Hu, W. De Coen, J. L. Newsted and J. P. Giesy, *Environ. Toxicol. Chem.*, 2003, **22**, 2639–2649.
98 M. J. Weiss-Errico, J. Miksovska and K. E. O'Shea, *Chem. Res. Toxicol.*, 2018, **31**, 277–284.
99 A. H. Karoyo, A. S. Borisov, L. D. Wilson and P. Hazendonk, *J. Phys. Chem. B*, 2011, **115**, 9511–9527.
100 L. R. S. Barbosa, M. G. Ortore, F. Spinozzi, P. Mariani, S. Bernstorff and R. Itri, *Biophys. J.*, 2010, **98**, 147–157.